Proceedings of the Eighteenth International Conference on
Civil, Structural and Environmental Engineering Computing
Edited by: P. Iványi, J. Kruis and B.H.V. Topping
Civil-Comp Conferences, Volume 10, Paper 3.2
Civil-Comp Press, Edinburgh, United Kingdom, 2025
ISSN: 2753-3239, doi: 10.4203/ccc.10.3.2
©Civil-Comp Ltd, Edinburgh, UK, 2025

Structural Topology Optimization Subjected to the Variance Constraint of Normal Deformation

D. Wu, T. Gao and W. Zhang

**Northwestern Polytechnical University,
China**

Abstract

This paper proposed an optimization method which improves the uniformity of normal deformation of local regions in the boundary of structure. Firstly, the variance of normal displacements is proposed as the measurement of the uniformity of normal deformation on a surface under small deformation conditions. And a topology optimization method based on the density method improving uniformity of normal deformation on surfaces is proposed by introducing variance of normal displacements into topology optimization problems. The relative sensitivity is calculated via adjoint method. Afterwards, the proposed method has been verified on a numerical case. The result of the numerical case implied that by using the proposed optimization method the uniformity of normal deformation on a surface is quantitively measured properly and effectively improved with a slight influence on global stiffness and acceptable extra cost on convergence.

Keywords: topology optimization, thermal protection structure, deformation control, nodal displacements, variance constraint, sensitivity analysis

1 Introduction

In decades, the optimization method has been developed as one of the most efficient approaches for lightweight structural design with multidisciplinary performance requirements. Recent progress and applications of topology optimization have been summarized in literature reviews[1-5], these achievements continue to improve the performance and practical applications of the topology optimization method.

Deformation control has been one of the key problems in topology optimization. A common and natural approach to control deformation is by controlling nodal displacements directly, Yang[6] established a multi-objective topology optimization model with stress and displacement constraints based on the ICM method. Single-point or multi-point displacement constrains were also introduced in the design-space adjusted optimization proposed by Rong[7] and NURBS-based SIMP method optimization proposed by Rodriguez[8]. In engineering practice, Maute[9] introduced a wing-tip displacement optimization constrain which effectively suppresses wing deformation in wing structure topology optimization. Since displacement constraints of large-scale points may lead to complexities in the iteration process, researchers have provided some approaches accordingly. Qiao[10] proposed an optimization method minimizing geometric average displacement, compared to compliance minimizing optimization, this method is more effective in minimizing displacement. Zuo[11] achieved a global constraint on displacement based on the BESO optimization method. The above deformation control methods are natural measurements for deformations but have difficulties in isolating rigid mode from displacement and thus are not able to measure deformation properly in some cases.

Another approach controls local deformation by controlling compliance, a commonly used measurement for structural stiffness in topology optimizations. It has been introduced as an optimization objective by Bendsøe[12], Nha Chu and Xie[13] with the ESO method, and Wang[14] with the level-set method. Similar quantities are introduced as measurements for local deformations, Zhu[15] introduced local strain energy as a measurement and optimization constraint for regional warping deformation in topology optimization, and Li[16] expanded this method by proposing AWE strain energy as a measurement for deformation of openings on structures, afterward, this method was developed into dynamic[17-19], nonlinear[20, 21], and electromagnetic[22, 23] fields. This kind of method is advantageous in efficiency in excluding rigid mode from total displacement and constructing optimization problems, but as an overall measurement of warping deformation strain energy lacks flexibility in controlling different patterns of deformation.

Therefore, this paper proposes a method aiming at enhancing the uniformity of normal deformation. In section 2, the variance of normal displacement (VND) is introduced as the measurement of the uniformity of normal deformation of a local region in the boundary of a structure. VND-controlled optimizations are formulated and sensitivity analysis for VND is conducted afterwards. In section 3, numerical examples including illustrative examples and engineer examples for validation of the proposed optimization method. Finally, concluding remarks are made in section 4.

2 Methods

In this section, a measurement for uniformity of normal deformation on local regions in boundary of the structure based on the variance of normal displacement is proposed and introduced into topology optimizations, sensitivity analysis of VND is conducted via adjoint method afterwards so that the VND controlled optimization method is completely formulated.

2.1 Measurement for uniformity of normal deformation

This work is motivated by engineering practices, the uniformity of normal deformation sometimes plays a significant row in the performance of structure. For example, the thermal protection structure in Figure 1 for aerospace vehicles consists of panels fixed on the frames which are tolerant to uniformed normal deformation but vulnerable to inconsistent normal deformation.

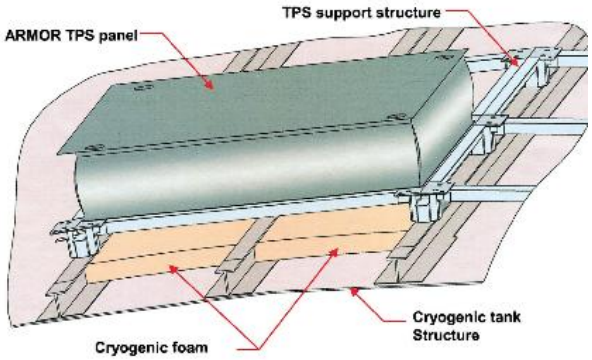

Figure 1: Typical TPS Structure on Aerospace Vehicles

Therefore, a topology optimization method aiming at enhancing the uniformity of normal deformation is proposed in this paper. To get a more illustrative view, the optimization problem is presented in Figure 2. Γ is a structural boundary on the global structure Ω is assigned as the surface region where the uniformity of normal deformation needs suppression.

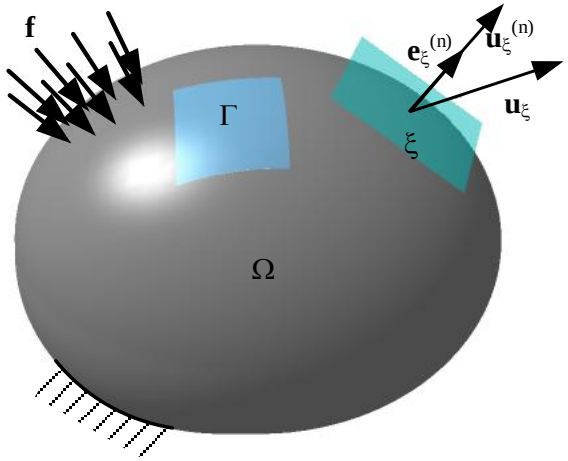

Figure 2: Structure for Optimization Problem

Let ξ be a point on the surface of Ω, the normal component of ξ is written as $u_\xi^{(n)}$, and displacements of all nodes on the surface Γ is written as $u_\Gamma^{(n)}$. Since normal deformation of Γ is determined by $u_\Gamma^{(n)}$, the variance of $u_\Gamma^{(n)}$ (VND) noted as $D\left(u_\Gamma^{(n)}\right)$, is defined as the quantitative measurement for uniformity of normal deformation on

the surface Γ . in a continuous structure, $D\left(u_{\Gamma}^{(n)}\right)$ is written as:

$$D\left(u_{\Gamma}^{(n)}\right)=\frac{1}{A}\iint_{\xi\in\Gamma}\left(u_{\xi}^{(n)}-\frac{1}{A}\iint_{\xi\in\Gamma}u_{\xi}^{(n)}da\right)^{2}da \tag{1}$$

where A is the area of Γ . In discrete FEM structure, $D\left(u_{\Gamma}^{(n)}\right)$ is written as

$$D(u_{\Gamma}^{(n)})=\frac{1}{m}\sum_{\xi\in\Gamma}(u_{\xi}^{(n)}-\overline{u_{\Gamma}^{(n)}})^{2} \tag{2}$$

where $\overline{u_{\Gamma}^{n}}$ is the average of the normal component of displacements of points on Γ :

$$\overline{u_{\Gamma}^{(n)}}=\frac{1}{m}\sum_{\xi\in\Gamma}u_{\xi}^{(n)} \tag{3}$$

By the definition above, the uniformity of normal deformation of Γ is measured by the VND of all nodes on Γ , shown in Figure 3 (a). For convenience in the optimization problem definition and efficiency in sensitivity analysis, another shrink method that measures the uniformity of normal deformation of Γ by the VND of key points on Γ , which is shown in Figure 3 (b), is proposed. In this paper, the distribution of key points on Γ is even and the density of key points is determined by the nature of specific optimization problems.

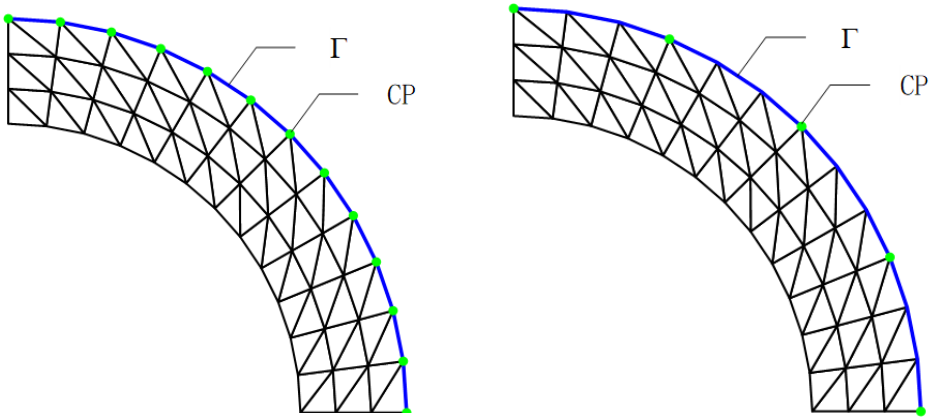

(a) All Nodes Controlled (b) Key Nodes Controlled

Figure 3: control methods for uniformity of normal deformation

2. 2 Formulation of VND Controlled Optimization

Classic topology optimization problem to find a configuration with minimum global compliance constrained by material volume is given by equation (4) where $\mathbf{x}$ is the vector composed of design variables x_i which is the pseudo-density of the corresponding element in the design domain, a lower bound $x_{\min}$ is assigned in purpose

of avoiding singularity of the stiffness matrix. Global compliance is retrieved by $C = \mathbf{U}^{\mathrm{T}}\mathbf{K}\mathbf{U}/2$ where $\mathbf{K}$ is a function of $\mathbf{x}$ while $\mathbf{U}$ is fetched by finite elements equation $\mathbf{f} = \mathbf{K}\mathbf{U}$, V is the volume of material in the design domain, it is also a function of $\mathbf{x}$ and is constrained by the maximum volume $V_{\max}$.

$$\begin{aligned} find: \quad & \mathbf{x} = (x_1, \cdots, x_n) \\ \min: \quad & C = \frac{1}{2}\mathbf{U}^{\mathrm{T}}\mathbf{K}\mathbf{U} \\ s.t.: \quad & \mathbf{f} = \mathbf{K}\mathbf{U} \\ & V \le V_{\max} \\ & 0 < x_{\min} \le x_i \le 1, (i = 1, \cdots, n) \end{aligned} \tag{4}$$

In this paper, two formulas of VND-constrained optimization are established, one is by adding an extra constraint on the upper bound of VND:

$$D(u_{\Gamma}^{(\mathrm{n})}) \le D_{\max} \tag{5}$$

to classic optimization which is given by equation (4) and the VND-constrained optimization given by equation (6):

$$\begin{aligned} find: \quad & \mathbf{x} = (x_1, \cdots, x_n) \\ \min: \quad & C = \frac{1}{2}\mathbf{U}^{\mathrm{T}}\mathbf{K}\mathbf{U} \\ s.t.: \quad & \mathbf{f} = \mathbf{K}\mathbf{U} \\ & V \le V_{\max} \\ & D(u_{\Gamma}^{(\mathrm{n})}) \le D_{\sup} \\ & 0 < x_{\min} \le x_i \le 1, (i = 1, \cdots, n) \end{aligned} \tag{6}$$

Another optimization is formulated by introducing the VND as the optimization objective and an additional upper bound on global compliance as an extra constraint which is given by equation (7):

$$\begin{aligned} find: \quad & \mathbf{x} = (x_1, \cdots, x_n) \\ \min: \quad & D(u_{\Gamma}^{(\mathrm{n})}) \\ s.t.: \quad & \mathbf{f} = \mathbf{K}\mathbf{U} \\ & V \le V_{\max} \\ & C \le C_{\max} \\ & 0 < x_{\min} \le x_i \le 1, (i = 1, \cdots, n) \end{aligned} \tag{7}$$

herein, $C_{\max}$ is the upper bound of global compliance.

For material interpolation, the SIMP model is used in this paper where penalization of Young's modulus for elements in the design domain is given by equation (8)

$$E_i = x_i^p E_0 \tag{8}$$

where E_0 is Young's modulus of the original material and p is the penalty factor which is prescribed at 3 in this work and the density penalization of material is given by equation (9)

$$\rho_i = x_i^p \rho_0 \tag{9}$$

where ρ_0 is the density of the original material.

2. 3 Sensitivity analysis

Sensitivities of gradient-based topology optimizers are derivatives of the optimization objective and constraints with respect of the design variables. As the sensitivity analysis for basic optimization problems including (4) is well-developed in numerous references (e.g. Bendsøe 1989; Sigmund 2001), the sole focus of sensitivity analysis here naturally turns to retrieving the derivative of $D(u_\Gamma^{(\mathrm{n})})$ to the design variable $\mathbf{x}$ and sensitivity analysis for global compliance C and volume V is skipped.

In this section $D(u_\Gamma^{(\mathrm{n})})$ is be transformed into matrix form for the convenience of sensitivity analysis. Let $\mathbf{D}_\Gamma$ be a m-ordered symmetric matrix given by equation (10)

$$\mathbf{D}_\Gamma = \begin{bmatrix} 1-\frac{1}{m} & -\frac{1}{m} & \cdots & -\frac{1}{m} \\ -\frac{1}{m} & \ddots & \ddots & \vdots \\ \vdots & \ddots & \ddots & -\frac{1}{m} \\ -\frac{1}{m} & \cdots & -\frac{1}{m} & 1-\frac{1}{m} \end{bmatrix} \tag{10}$$

let $\mathbf{d}$ be a vector given by equation (11)

$$\mathbf{d}_\Gamma = \begin{bmatrix} u_{\gamma_1}^{(\mathrm{n})} - \overline{u_\Gamma^{(\mathrm{n})}} \\ \cdots \\ u_{\gamma_m}^{(\mathrm{n})} - \overline{u_\Gamma^{(\mathrm{n})}} \end{bmatrix} = \mathbf{D}_\Gamma \xi_\Gamma^{(\mathrm{n})} \tag{11}$$

where $\xi_\Gamma^{(\mathrm{n})} = \left[u_{\gamma_1}^{(n)}, \quad \cdots, \quad u_{\gamma_m}^{(n)} \right]^{\mathrm{T}}$, and equation (2) is written as

$$D(u_\Gamma^{(\mathrm{n})}) = \frac{1}{m} \sum_{j \in \Gamma} (u_j^{(\mathrm{n})} - \overline{u_\Gamma^{(\mathrm{n})}})^2 = \frac{1}{m} \mathbf{d}_\Gamma^{\mathrm{T}} \mathbf{d}_\Gamma = \xi_\Gamma^{(\mathrm{n})\mathrm{T}} \mathbf{D}_\Gamma^{\mathrm{T}} \mathbf{D}_\Gamma \xi_\Gamma^{(\mathrm{n})} \tag{12}$$

where $\xi_\Gamma^{(\mathrm{n})}$ is furtherly expressed by global displacement $\mathbf{u}$. Firstly, the normal component of displacement is calculated as below. As is shown in Figure 2, at point

γ_k, $\mathbf{u}_{\gamma_k}$ is the displacement vector, $\mathbf{e}_{\gamma_k}^{(\mathrm{n})}$ is the normal unit vector, and $\mathbf{u}_{\xi}^{(\mathrm{n})}$ is normal displacement. By projecting $\mathbf{u}_{\gamma_k}$ on $\mathbf{e}_{\gamma_k}^{(\mathrm{n})}$, $\mathbf{u}_{\xi}^{(\mathrm{n})}$ is given by equation (13)

$$\mathbf{u}_{\gamma_k}^{(\mathrm{n})}=u_{\gamma_k}^{(\mathrm{n})}\mathbf{e}_{\gamma_k}^{(\mathrm{n})} \tag{13}$$

multiplied by $\mathrm{e}_{\gamma_k}^{(\mathrm{n})\mathrm{T}}$ on both sides of the equation, (13) is transformed into

$$u_{\gamma_k}^{(\mathrm{n})}=\mathbf{e}_{\gamma_k}^{(\mathrm{n})\mathrm{T}}\mathbf{u}_{\gamma_k} \tag{14}$$

In discrete structure Ω, $\mathbf{u}_{\gamma_k}$, the translational displacement of the node γ_k is written as:

$$\mathbf{u}_{\gamma_k}=\mathbf{S}_{\gamma_k}\mathbf{u} \tag{15}$$

herein $\mathbf{S}_{\gamma_k}$ is a $3\times 6n$ extraction matrix whose element s_{jk} is:

$$s_{jk}=\begin{cases}1 & (j,k)=\left\{\left(1,\gamma_k+1\right),\left(2,\gamma_k+2\right),\left(3,\gamma_k+3\right)\right\}\\ 0 & else\end{cases} \tag{16}$$

Taking (15) into (14), $u_{\gamma_k}^{(\mathrm{n})}$ is given by equation (17)

$$u_{\gamma_k}^{(\mathrm{n})}=\mathbf{e}_{\gamma_k}^{(\mathrm{n})}\mathbf{u}_{\gamma_k}=\mathbf{e}_{\gamma_k}^{(\mathrm{n})\mathrm{T}}\mathbf{S}_{\gamma_k}\mathbf{u} \tag{17}$$

and $\mathbf{S}^{(\mathrm{n})}$ is therefore given by equation (18)

$$\mathbf{S}_{\Gamma}^{(\mathrm{n})}=\begin{bmatrix}\mathbf{e}_{\gamma_1}^{(\mathrm{n})\mathrm{T}}\mathbf{S}_{\gamma_1}\\ \cdots\\ \mathbf{e}_{\gamma_m}^{(\mathrm{n})\mathrm{T}}\mathbf{S}_{\gamma_m}\end{bmatrix} \tag{18}$$

and $\xi_{\Gamma}^{(\mathrm{n})}$ is written by the global displacement $\mathbf{u}$ multiplied by a constant matrix, written as:

$$\xi_{\Gamma}^{(\mathrm{n})}=\begin{bmatrix}u_{\gamma_1}^{(\mathrm{n})}\\ \cdots\\ u_{\gamma_m}^{(\mathrm{n})}\end{bmatrix}=\begin{bmatrix}\mathbf{e}_{\gamma_1}^{(\mathrm{n})\mathrm{T}}\mathbf{S}_{\gamma_1}\mathbf{u}\\ \cdots\\ \mathbf{e}_{\gamma_m}^{(\mathrm{n})\mathrm{T}}\mathbf{S}_{\gamma_m}\mathbf{u}\end{bmatrix}=\mathbf{S}_{\Gamma}^{(\mathrm{n})}\mathbf{u} \tag{19}$$

and ， (12) is written as.

$$D(u_{\Gamma}^{(\mathrm{n})})=\frac{1}{m}\xi_{\Gamma}^{(\mathrm{n})\mathrm{T}}\mathbf{D}_{\Gamma}^{\mathrm{T}}\mathbf{D}_{\Gamma}\xi_{\Gamma}^{(\mathrm{n})}=\frac{1}{m}\mathbf{u}^{\mathrm{T}}\mathbf{S}_{\Gamma}^{(\mathrm{n})\mathrm{T}}\mathbf{D}_{\Gamma}^{\mathrm{T}}\mathbf{D}_{\Gamma}\mathbf{S}_{\Gamma}^{(\mathrm{n})}\mathbf{u} \tag{20}$$

The sensitivity of $D(u_{\Gamma}^{(\mathrm{n})})$ to the design variables x_j is:

$$\frac{\partial D(u_{\Gamma}^{(\mathrm{n})})}{\partial x_i}=\frac{2}{m}\mathbf{u}^{\mathrm{T}}\mathbf{S}_{\Gamma}^{(\mathrm{n})\mathrm{T}}\mathbf{D}_{\Gamma}^{\mathrm{T}}\mathbf{D}_{\Gamma}\mathbf{S}_{\Gamma}^{(\mathrm{n})}\frac{\partial \mathbf{u}}{\partial x_i} \tag{21}$$

the differentiation of the finite element equilibrium $\mathbf{f}=\mathbf{K}\mathbf{u}$ by x_j, $\partial\mathbf{u}/\partial x_j$ is noted as

$$\frac{\partial \mathbf{u}}{\partial x_j}=\mathbf{K}^{-1}(\frac{\partial \mathbf{f}}{\partial x_j}-\frac{\partial \mathbf{K}}{\partial x_j}\mathbf{u}) \tag{22}$$

Substituting $\partial\mathbf{u}/\partial x_j$ in (21), $\partial D(\mathbf{u}_{\Gamma}^{n})/\partial x_j$ is furtherly derived as

$$\frac{\partial D(u_{\Gamma}^{(n)})}{\partial x_i}=\frac{2}{m}\mathbf{u}^{\mathrm{T}}\mathbf{S}_{\Gamma}^{(\mathrm{n})\mathrm{T}}\mathbf{D}_{\Gamma}^{\mathrm{T}}\mathbf{D}_{\Gamma}\mathbf{S}_{\Gamma}^{(\mathrm{n})}\mathbf{K}^{-1}(\frac{\partial \mathbf{f}}{\partial x_j}-\frac{\partial \mathbf{K}}{\partial x_j}\mathbf{u}) \tag{23}$$

To avoid the complicated process of calculating $\mathbf{K}^{-1}$, the adjoint method is applied in this paper. Introducing

$$\begin{aligned}\Lambda^{\mathrm{T}}&=\frac{2}{m}\mathbf{u}^{\mathrm{T}}\mathbf{S}_{\Gamma}^{(\mathrm{n})\mathrm{T}}\mathbf{D}_{\Gamma}^{\mathrm{T}}\mathbf{D}_{\Gamma}\mathbf{S}_{\Gamma}^{(\mathrm{n})}\mathbf{K}^{-1}\\ \mathbf{q}&=\frac{2}{m}\mathbf{u}^{\mathrm{T}}\mathbf{S}_{\Gamma}^{(\mathrm{n})\mathrm{T}}\mathbf{D}_{\Gamma}^{\mathrm{T}}\mathbf{D}_{\Gamma}\mathbf{S}_{\Gamma}^{(\mathrm{n})}\end{aligned} \tag{24}$$

where Λ artificial adjoint vector and $\mathbf{q}$ is artificial load, the adjoint vector Λ is then computed by an extra finite element equilibrium

$$\mathbf{q}=\mathbf{K}\Lambda \tag{25}$$

and the sensitivity of $D\left(u_{\Gamma}^{(\mathrm{n})}\right)$ to x_i, $\partial D(u_{\Gamma}^{(\mathrm{n})})/\partial x_i$ is therefore given by equation (26)

$$\frac{\partial D(u_{\Gamma}^{(\mathrm{n})})}{\partial x_j}=\Lambda^{\mathrm{T}}(\frac{\partial \mathbf{f}}{\partial x_j}-\frac{\partial \mathbf{K}}{\partial x_j})\mathbf{u} \tag{26}$$

where $\partial\mathbf{f}/\partial x_j$ and $\partial\mathbf{K}/\partial x_j$ is calculated through predefined analytical expression or prescribed numerical data.

3 Numerical results

In this section, A 2D MBB beam example is investigated to validate if the proposed VND parameter is effective as a measurement for uniformity of normal deformation and the effectiveness of the proposed VND controlled optimizations. See Figure 4 the structure is 500mm×100mm in size and discretized into 4-node square plane elements with the size of $1\mathrm{mm}\times1\mathrm{mm}$. The top edge of the design domain with a gap of 5mm to the left end is prescribed VND-controlled region, the left edge of the structure is fixed, and a concentrated force of 50N is applied at the midpoint on the right edge. For material, the elastic modulus is 210GPa, and the Poisson's ratio is 0.33.

A classic topology optimization problem, which is given by equation (4), is first applied as the baseline for the proposed VND-controlled optimization. The objective of the optimization problem is minimizing global compliance with an upper bound on volume of 30%. The optimization problem converged after 42 iterations, the VND of

the optimized design is $2.602\times10^{-7}\,\mathrm{mm}^2$ and the global compliance is $5.247\times10^{-2}\,\mathrm{mJ}$.

Based on the classic optimization, VND-constrained optimization introduced an extra constraint on the upper bound of VND of $1.301\times10^{-8}\,\mathrm{mm}^2$ (5% of classic design) with objective and other constraints unchanged. This optimization converged after 52 iteration steps with VND decreased to $1.144\times10^{-8}\,\mathrm{mm}^2$ and the global compliance consequently increased to 5.571×10^{-2} mJ (106.18% of the classic design) which implied that the global stiffness deteriorated in exchange for enhancement of normal deformation uniformity of the top edge.

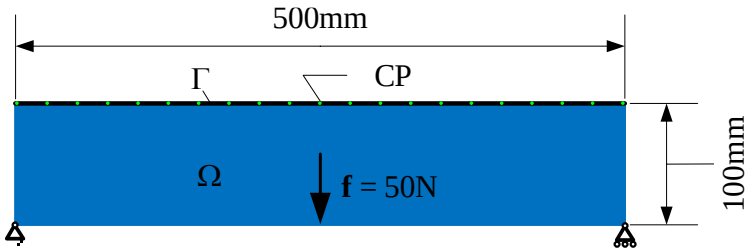

Figure 4: MBB Beam

VND-minimized optimization assigned VND of the top edge as the optimization objective, and an extra constraint on global compliance of 5.571×10^{-2} mJ (Compliance of the VND constraint design) is introduced with a constraint on the upper bound of the volume of 30%. This optimization converged feasibly with VND decreased to 7.853×10^{-8} mJ after 300 steps.

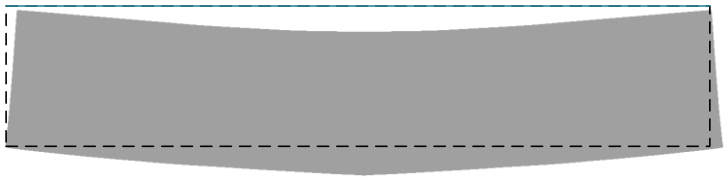

(a) Classic Design

(b) VND Constrained Design

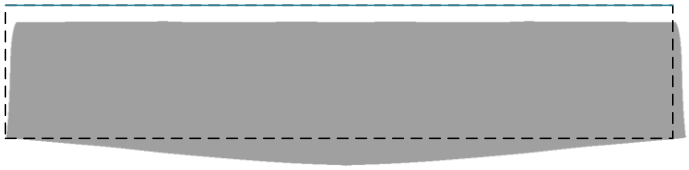

(c) VND Minimized Design

Figure 5: Scaled Deformation Pattern

The scaled deformation figure is shown in Figure 5. It is obvious that both VND-constrained design and VND-minimized design have effectively enhanced the uniformity of normal deformation on the prescribed region and the uniformity of normal deformation improves as VND in optimized design declines, which implies that VND of a prescribed region functioned well as the measurement of uniformity of normal deformation.

The optimized design's material layouts are shown in Figure 6, 2 of the proposed VND-controlled optimizations has changed the transmission path in both locally and globally compare to the classic optimization, and have converged on clear transmission paths which are preferable for engineering practice.

(a) Classic Optimization

(b) VND-Minimized Optimization

(c) VND-Minimized Optimization

Figure 6: Material Layouts

This numerical case demonstrated that the VND functioned well as the measurement of uniformity, and the proposed VND-controlled optimizations are capable of improving the uniformity of prescribed regions for given case.

4 Conclusions

This paper has proposed a VND controlled optimization method aiming at enhancing normal deformation uniformity on structural surfaces or edges. By introducing variance of normal displacements of nodes on local region of structural boundary, the uniformity of normal deformation under small displacement conditions is quantitively measured and constrained or minimized in corresponding optimizations.

Numerical tests and comparisons with classic topology optimizations demonstrated that the uniformity of normal deformation on the surface or edge has been improved

successfully with acceptable sacrifice of global stiffness in both illustrative example and engineering case.

Acknowledgements

This paper is supported by Defense Industrial Technology Development Program JCKY2022205B020.

References

[1] T.P. Ribeiro, L.F.A. Bernardo, J.M.A. Andrade, "Topology Optimisation in Structural Steel Design for Additive Manufacturing", Applied Sciences, 11(5), 2021, 10.3390/app11052112

[2] J. Zhu, H. Zhou, C. Wang, et al., "A review of topology optimization for additive manufacturing: Status and challenges", Chinese Journal of Aeronautics, 2020, 10.1016/j.cja.2020.09.020

[3] J. Zhu, W. Zhang, L. Xia, "Topology Optimization in Aircraft and Aerospace Structures Design", Archives of Computational Methods in Engineering, 23(4), 595-622, 2015, 10.1007/s11831-015-9151-2

[4] G.I.N. Rozvany, "Aims, scope, methods, history and unified terminology of computer-aided topology optimization in structural mechanics", Structural and Multidisciplinary Optimization, 21(2), 90-108, 2014, 10.1007/s001580050174

[5] O. Sigmund, K. Maute, "Topology optimization approaches", Structural and Multidisciplinary Optimization, 48(6), 1031-1055, 2013, 10.1007/s00158-013-0978-6

[6] D. Yang, Y. Sui, Z. Liu, et al., "Topology optimization design of continuum structures under stress and displacement constraints", Applied Mathematics and Mechanics, 21(1), 19-26, 2000, 10.1007/bf02458535

[7] J.H. Rong, J.H. Yi, "A structural topological optimization method for multi-displacement constraints and any initial topology configuration", Acta Mechanica Sinica, 26(5), 735-744, 2010, 10.1007/s10409-010-0369-9

[8] T. Rodriguez, M. Montemurro, P. Le Texier, et al., "Structural Displacement Requirement in a Topology Optimization Algorithm Based on Isogeometric Entities", Journal of Optimization Theory and Applications, 184(1), 250-276, 2019, 10.1007/s10957-019-01622-8

[9] K. Maute, M. Allen, "Conceptual design of aeroelastic structures by topology optimization", Structural and Multidisciplinary Optimization, 27(1-2), 27-42, 2004, 10.1007/s00158-003-0362-z

[10] H. Qiao, S. Liu, "Topology optimization by minimizing the geometric average displacement", Engineering Optimization, 45(1), 1-18, 2013, 10.1080/0305215x.2012.654789

[11] Z.H. Zuo, Y.M. Xie, X. Huang, "Evolutionary Topology Optimization of Structures with Multiple Displacement and Frequency Constraints", Advances in Structural Engineering, 15(2), 359-372, 2012, 10.1260/1369-4332.15.2.359

[12] M.P. Bendsøe, "Optimal shape design as a material distribution problem", Structural Optimization, 1(4), 193-202, 1989, 10.1007/bf01650949

[13] D. Nha Chu, Y.M. Xie, A. Hira, et al., "On various aspects of evolutionary structural optimization for problems with stiffness constraints", Finite Elements in Analysis and Design, 24(4), 197-212, 1997, 10.1016/s0168-874x(96)00049-2
[14] M.Y. Wang, X. Wang, D. Guo, "A level set method for structural topology optimization", Computer Methods in Applied Mechanics and Engineering, 192(1-2), 227-246, 2003, 10.1016/s0045-7825(02)00559-5
[15] J. Zhu, Y. Li, W. Zhang, et al., "Shape preserving design with structural topology optimization", Structural and Multidisciplinary Optimization, 53(4), 893-906, 2015, 10.1007/s00158-015-1364-3
[16] Y. Li, J.H. Zhu, W.H. Zhang, et al., "Structural topology optimization for directional deformation behavior design with the orthotropic artificial weak element method", Structural and Multidisciplinary Optimization, 57(3), 1251-1266, 2017, 10.1007/s00158-017-1808-z
[17] Y. Wang, J. Zhu, Y. Li, et al., "Shape preserving design with topology optimization for structures under harmonic resonance responses", Structural and Multidisciplinary Optimization, 65(5), 2022, 10.1007/s00158-022-03218-9
[18] O.M. Silva, F. Valentini, E.L. Cardoso, "Shape and position preserving design of vibrating structures by controlling local energies through topology optimization", Journal of Sound and Vibration, 515(2021, 10.1016/j.jsv.2021.116478
[19] M.S. Castro, O.M. Silva, A. Lenzi, et al., "Shape preserving design of vibrating structures using topology optimization", Structural and Multidisciplinary Optimization, 58(3), 1109-1119, 2018, 10.1007/s00158-018-1955-x
[20] J. Zhu, Y. Li, F. Wang, et al., "Shape preserving design of thermo-elastic structures considering geometrical nonlinearity", Structural and Multidisciplinary Optimization, 61(5), 1787-1804, 2020, 10.1007/s00158-020-02532-4
[21] Y. Li, J. Zhu, F. Wang, et al., "Shape preserving design of geometrically nonlinear structures using topology optimization", Structural and Multidisciplinary Optimization, 59(4), 1033-1051, 2019, 10.1007/s00158-018-2186-x
[22] F. Chen, J. Zhu, W. Zhang, "Radar cross section minimization for step structures using topology optimization", Structural and Multidisciplinary Optimization, 65(2), 2022, 10.1007/s00158-021-03110-y
[23] F. Chen, J. Zhu, X. Du, et al., "Shape preserving topology optimization for structural radar cross section control", Chinese Journal of Aeronautics, 35(6), 198-210, 2022, 10.1016/j.cja.2021.10.014